Country distancing increase reveals the effectiveness of travel restrictions in stopping COVID-19 transmission

Lu Zhong
Rensselaer Polytechnic Institute
Mamadou Diagne
Rensselaer Polytechnic Institute
Weiping Wang
Beijing Jiaotong University
Jianxi Gao (gaoj8@rpi.edu)
Rensselaer Polytechnic Institute https://orcid.org/0000-0002-3952-208X

Physical Sciences - Article

Keywords: travel restrictions, COVID-19, country distancing, non-pharmaceutical interventions

Posted Date: September 11th, 2020

DOI: https://doi.org/10.21203/rs.3.rs-75264/v1

Country distancing increase reveals the effectiveness of travel restrictions in stopping COVID-19 transmission

Lu Zhong,[1] Mamadou Diagne,[1*] Weiping Wang,[2] Jianxi Gao[3,4*]

[1]*Department of Mechanical, Aerospace, and Nuclear Engineering, Rensselaer Polytechnic Institute, Troy, NY 12180*

[2]*Institute of Transportation Systems Science and Engineering, Beijing Jiaotong University, Beijing, China 100044*

[3]*Department of Computer Science, Rensselaer Polytechnic Institute, Troy, NY 12180*

[4]*Network Science and Technology Center, Rensselaer Polytechnic Institute, Troy, NY 12180*

Non-pharmaceutical interventions are the current central strategy to stop transmitting the novel coronavirus disease (COVID-19) globally. Despite remarkably successful approaches in predicting the ongoing pandemic's spatiotemporal patterns, we lack an intrinsic understanding of the travel restrictions' efficiency and effectiveness. We fill this gap by examining the countries' closeness based on disease spread using country distancing that is analogical to the effective resistance in series and parallel circuits and captures the propagation backbone tree from the outbreak locations globally. Our method estimates that 53.6% of travel restrictions as of June 1, 2020, are ineffective. Our analytical results unveil that the optimal and coordinated travel restrictions postpone per geographical area by 22.56 [95% credible interval (CI), 18.57 to 26.59] days of the disease's arrival time and protect the world by reducing 1,872,295 (95% CI, 216,029 to 23,606,312) infected cases till June 1, 2020, which are signif-

icantly better than the existing travel restrictions achieving 12.87 (95% CI, 10.59 to 15.17) days of arrival time delay and 861,867 (95% CI, 238,250 to 3,879,638) infected cases reduction. Our approach offers a practical guide that indicates when and where to implement travel restrictions, tailed to the real-time national context.

The COVID-19, with 19,718,030 confirmed cases and 728,013 deaths worldwide, as of August 10, 2020, was first reported to the WHO (World Health Organization) on December 31, 2019[1,2]. Today's high population density and high volume, speed, and non-locality of human mobility provide perfect conditions for epidemic spreading[3–6], and simultaneously raise challenges related to the development non-pharmaceutical intervention strategies on the timescale modern diseases spread[7–9]. Specifically, through the global mobility network (GMN), mainland China introduced 288 infected cases to other geographical areas from January 3, 2020, to February 13, 2020[10,11]. As COVID-19 was declared a pandemic on March 11, 2020, more than half of the geographical areas was infected. The geographical areas exposed to massive airline transits from different infected countries are currently in high importation risk[8]. For example, the virus in the United States was mainly imported from European countries, including France, Austria, and the Netherlands[12,13], which was experiencing an exponentially growing number of infected cases with 4,951,851 confirmed cases and 53,893 deaths till August 10, 2020.

Although the practice of quarantine and social distancing protocols can drastically reduce the virus' propagation locally[14], the global pandemic patterns of COVID-19 are shaped by the GMN, which determines when and where the disease arrives globally[15,16]. Consequently, the straightfor-

ward way for diminishing the international importation of COVID-19 is to impose radical travel restrictions (i.e., entry ban, global travel ban, and lockdown)[17,18], which enable to shrink the entry of airline passengers. According to our dataset, 187 geographical areas imposed the entry ban, 111 geographical regions imposed the global travel ban, and 38 geographical areas imposed the full lockdown to prevent their citizens and tourists from traveling overseas as of June 1, 2020[19,20]. However, researchers demonstrated that these travel restrictions were only effective at the beginning of an outbreak[21]. Moreover, they would interrupt the healthcare aid and technical support, disrupt businesses, and cause extensive and profound social and economic damage[22,23]. Therefore, it is crucial to assess and impose effective travel restrictions to avoid uncoordinated government responses to COVID-19[24], leading to a substantial unnecessary cost.

Measuring the travel restrictions' effectiveness often relies on the specific epidemic models[25–27], which require accurate estimation of the disease's epidemiological parameters, such as the basic reproductive number (R_0). However, the parameter estimations are often unreliable due to the daily changing under-reported cases and various errors arising from the lack of diagnosis tests[7,28–30]. Furthermore, these models are hard to calibrate by the virtue of incomplete information (i.e., partial network topology[31] or unknown dynamics[17,32]). Overall, it is unclear how much details are required to achieve a certain level of predictive accuracy. Human mobility plays a crucial role in understanding the hidden spatiotemporal spreading patterns and enables us to predict the arrival time[15] and estimate the number of infected cases[33] without knowing the epidemiological parameters. It is remarkable that despite the complex topology of the mobility network, a dominant trajectory defined as the effective distance[15] can always be identified from the outbreak location (OL)

to the target geographical area by discarding other redundant connections. This method reliably predicts the arrival time and epidemic wavefront without knowing the epidemiological parameters, which has already been demonstrated in both the 2009 H1N1 pandemic and the 2003 SARS epidemic. On the other hand, the OL's aggregate mobility outflow has also been a vital predictor for the cumulative number of infections in the destination location[33], validated by the Wuhan's outflow to each prefecture in mainland China. Despite advances of both approaches and their follow-up methods[8,34,35], they are more suitable for the early stage of the pandemic of COVID-19 than the late stage when multiple OLs arise, increasing the level of complexity that promotes the needs of new mathematical tools.

Global Disease Transmission Law and Country Distancing. We test the international spreading of the COVID-19 on the GMN (see Fig. 1A and Tab. S1) provided by the Official Aviation Guide. We define GMN as $G = (N, E, F)$, N denotes a set of countries, dependent territories, and special areas of geographical interest (geographical areas) and $|N| = 250$. Besides, E represents the airline link set, and F_{mn} ($F_{mn} \in F$) expresses the airline passenger influx from area n to the area m. For a complex GMN with a single OL, the diseases may propagate to a geographical area through distinct paths, the shortest of which predicts the arrival time to the destination[15]. For area n and its connected area m, their effective distance is $d_{m|n} = 1 - \log P_{mn}$, indicating that a larger fraction of air travel P_{mn} ($P_{mn} = \frac{F_{mn}}{\sum_k F_{km}}$) means a smaller distance, and vice versa. Then, for an arbitrary area that can be reached by n through a path τ, the effective distance is the sum of effective lengths along the links of the shortest path, $d_{m|n} = \min_{\tau} \sum_{(i,j)\in\tau} d_{j|i}$. We call this se-

ries connection law because it is analogical to the *effective resistance* in series circuits defined as $R = \sum_i R_i$, where R_i is the resistance that is connected along a chain.

The number of OLs grows (see Fig. S2), which escalates importation risk for the other geographical areas, and simultaneously dwindle geographical areas' distance to the risky sources. Examining the closeness to all existing OLs, we develop the parallel connection law for global disease transmission. For example, the disease propagates from two OLs, n and c, to the destination geographical area, m, with effective distance $d_{m|n}$, and $d_{m|c}$ respectively. The overall likelihood of transmitting from both OLs satisfies $e^{d_{m|\{n,c\}}} \propto \frac{1}{\frac{1}{e^{d_{c|n}}}+\frac{1}{e^{d_{m|n}}}}$ (see supplementary information). This process is similar to the *effective resistance* in parallel circuits that $R = \frac{1}{\frac{1}{R_n}+\frac{1}{R_c}}$. For the general case, we derive the series and parallel connection law for global disease transmission and formulate it as country distancing (see Fig. 1B)

$$D_{m|N_I} = log\frac{M}{\sum_{n_i \in N_I} \frac{1}{e^{d_{m|n_i}}}} \tag{1}$$

where $N_I = \{i|\forall i \in N \& I_i^a > I_{\mathrm{c}}\}$ is the OL set at time t. As it is observed that the confirmed cases of COVID-19 rises exponentially after the 100th case is confirmed[36], we set the threshold I_{c} equal to 100. Here, I_i^a is the active confirmed infected cases at area i, and $M(M = 250)$ is the total number of geographical areas. See supplementary information [Eqs. (S1)-(S10)] for the details about Eq. (1). Note that a large set of OLs may lead to a small country distancing, and a larger portion of passenger influx leads to smaller effective distance and further may lead to a smaller country distancing.

Two fundamental properties describe the main spread patterns of the COVID-19 pandemic:

the arrival time (T_m) and the infected cases (I_m) in an arbitrary geographical area m. Increasing evidence shows that human mobility determines arrival times[8,15,35] and infected cases[33] when there is only one OL. However, these approaches are not suitable for the presence of multiple OLs because it is unclear how each OL contributes to the arrival time and infected cases in a geographical area. Our approach compresses multiple OLs to a single one and calculates the corresponding effective mobility using the series and parallel connection law for global disease transmission. As mass undetected, missing, undiagnosed, or unreported COVID-19 cases result in biased arrival times and infected cases in the collected real-world dataset[28,29], we simulate the spread of COVID-19 by adopting the meta-population susceptible-infected-recovered (SIR) model[37] with the given epidemiological parameters of COVID-19[38]. We surprisingly find that country distancing generates linear relationships with the simulated arrival times and the logarithm of the simulated infected cases with $R^2 > 0.8$, regardless of the number of outbreak locations (see Fig. S2-S4),

$$T_m = v_{N_I} \times D_{m|N_I} + v_{0N_I} \tag{2}$$

$$log(I_m) = u_{N_I} \times D_{m|N_I} + u_{0N_I} \tag{3}$$

where v_{N_I} and u_{N_I} are the slopes, respectively, representing the rates of change of arrival times/infected cases relative to country distancing.

Effectiveness and Efficiency of Travel Restrictions. Until June 1, 2020, 625 travel restrictions have been imposed (see Tab. S2 and Fig. S5), categorized into three types, i.e., entry ban, global travel ban, and lockdown. As illustrated in Fig. 1C [See Eqs. S(15)-(S17)], for the travel restrictions imposed by area n^s (marked in red circle), we assume that the entry ban only reduces the

passenger influx to banned areas from n^s with strength $\alpha = 50\%$; the global travel ban reduces the passenger influx from all neighbor areas to enter n^s with strength $\beta = 75\%$; the lockdown reduces the passenger influx entering/leaving n^s with strength $\gamma = 90\%$ for full lockdown. The entry ban implemented by the United States to mainland China on January 31, 2020, when mainland China is the only OL, is an illustrative example. By restricting passengers from mainland China entering the United States, the entry ban indirectly helps 29 areas (red square dot in Fig. 1D) by distancing them from the OL in the shortest path tree with a total of 15.95 *country distancing increase*. In order to assess the robustness of evaluation, we estimate the slopes for linear correlations for different OLs, and derive the generic slopes with 95% confidence interval, i.e., $\bar{v}$ ($\bar{v} = 5.37$ [95% CI, 4.42 to 6.63)] and $\bar{u}$ [$\bar{u} = -2.84$ (95% CI, -3.42 to -2.26)]. Given the slopes, the *country distancing increase* ("vertical change" in Fig. 1F) in the each area could be mapped to the corresponding ATD and ICR ("horizontal change" in Fig. 1F) by Eqs. (S18)-(S27), and further their upper and lower limits.

An overview of geographical areas' *country distancing increase* caused by travel restrictions' is shown in Fig. 2A. Through all existing travel restrictions, 33.7% of passenger influx is reduced from GMN, the arrival times of the virus in the world are delayed by 12.87 (95% CI, 10.59 to 15.17) days in average, and infected cases are reduced with 861,867 (95% CI, 238,250 to 3,879,638) cases. However, about 53.6% of them are ineffective, resulting in zero *country distancing increase* (see Tab. S3, Fig. S6-S8). Fig. 2B-C shows the left 46.4% travel restrictions' effectiveness and efficiency by representing the travel restrictions' ATD/ICR against the cost of losing passenger influx. The means of lost passenger influx (vertical line) and the ATD/ ICR (horizontal line) divide

the travel restrictions into four blocks, i.e., effective and efficient block (top left), effective and inefficient block (top right), ineffective and efficient block (bottom left), and ineffective and inefficient block (bottom right). Besides the one imposed by mainland China, the lockdowns imposed by New Zealand (@NZ), South Africa (@ZA) produce crucial ATD for the world. Concurrently, lockdowns established by Italy (@IT), Turkey (@TR), Spain (@ES), and global travel ban enforced by Turkey (*TR) carry about significant ICR for the world. However, these extreme travel restrictions also increase the economic burden with a high lost passenger influx. Several travel restrictions, e.g., the entry ban imposed by the United States (US-CN), Hong Kong (HK-CN), and Italy (IT-CN) to mainland China and the lockdown prescribed by Nepal (@CN), produces comparable ATD or ICR but with much fewer loss of passenger influx. Moreover, 553 (88.48%) travel restrictions generate less than 0.01 days of ATD and less than 1000 cases of ICR for the world, suggesting the ineffectiveness of travel restrictions.

Fig. 2 indicates that entry bans to the OLs are most effective in distancing themselves and their descendants in the shortest-path tree than to other areas, such as South Korea, Japan, Iran, and Schengen Areas. Specifically, the United States, Netherlands, Australia, and Russia, imposed effective entry bans to mainland China, as shown in Fig. 1D and Fig. 2B-C. The findings suggest that the travel restrictions imposed by the areas with more descendant areas in the shortest path tree are more effective in distancing the world from coronavirus's importation risk. The OLs, who are the sources of the shortest-path tree, have the most significant influence. By imposing the national lockdown on February 8, 2020, mainland China leads to 9.89 (95% CI, 8.14 to 11.66) days of ATD per geographical area and 552,883 (95% CI, 118,919 to 2,669,095) ICR in total, representing

76.8% of ATD and 64.1% of ICR generated by all travel restrictions. However, as the number of OLs grows, the areas' country distancing drops, substantial effort causes relatively smaller and even tiny *country distancing increase*. For example, Italy, one of the 83 sources of the shortest path tree, imposed the national lockdown on March 23, 2020. This lockdown leads to 0.002 (95% CI, 0.002 to 0.003) days of ATD per geographical area and 68,563 (95% CI, 37,863 to 121,222) cases of ICR in total, accounting for nearly 0% of ATD and 7.9% of ICR generated by all travel restrictions. Our results indicate that two factors determine the effectiveness of travel restrictions. One is the position of a geographical area that imposed travel restrictions on the shortest-path tree; another is the implementation date. Insufficient consideration of both two factors leads to ineffectiveness and further inefficiency of travel restrictions.

Optimal and Coordinated Travel Restrictions. We find that most of the existing travel restrictions are inefficient for two reasons: (1) the travel restrictions are imposed by geographical areas in an uncoordinated way out of self-interest, failing to contribute to global good; (2) the sole travel restriction is not enacted in optimal time and optimal locations for the most significant self-interest. Furthermore, these inefficient travel restrictions have created a substantial unnecessary loss of passenger influx, ultimately damaging the global economy and social stability[23], promoting us to design the strategical plans of when and where to impose each travel restriction, tailed to the real-time national context. Our coordinated travel restrictions can inflict the same amount of airlines as the existing travel restrictions but dramatically increase the country distancing and consequently increase ATD and ICR. Specifically, we formulate it as a bi-objective optimization

problem: maximizing the travel restrictions' *country distancing increase* and minimizing the loss of airline passenger influx in GMN [see Eq. (S28)].

By using the Non-dominated Sorting Genetic Algorithm (NSGA-II), we obtain non-dominated solutions for each travel restriction and present the approximate optimal solution, which has the largest *country distancing increase* in Fig. 3. Our numerical results show that the coordinated travel restrictions significantly outperform the existing travel restrictions in the three features, i.e., lost passenger influx, the average ATD, and the total ICR. As shown in Fig. 3A-C, the coordinated travel restrictions reach the ATD of average 22.56 days (95% CI, 18.57 to 26.59), with 25.12% of lost passenger influx. The ICR of the coordinated travel restrictions is 1,872,295 (95% CI, 216,029 to 23,606,312) cases, indicating an additional 16.67% of ICR till June 1, 2020. Unlike the existing travel restrictions suggesting that mainland China contributes most of ATD and ICR for the world, the coordinated travel restrictions work as a "whole-of-government" and "whole-of-society" approach with many geographical areas contributing substantially to an increase of ATD and ICR for the world[39]. As shown in Fig. 3D, mainland China occupies the small portions of ATD and ICR contribution, declining to 4.68% and 3.39%, respectively, from 76.8 % and 64.1% when a coordinated approach is adopted. Concurrently, other geographical areas contribute more when using a coordinated approach. For example, France's portion of ATD and ICR contribution could rise to 4.2% and 44.5%, respectively, from 0%. The United Kingdom's contribution to ATD and ICR could rise to 2.5% and 5.2%, respectively, from 0%.

Next, we examine when is the best time to impose travel restrictions by testing the differences

of ATD and ICR if the selected travel restrictions are imposed d days earlier ($d < 0$) or later ($d > 0$) than their original occurrence date in Fig. 3E-F. To avoid the intertwined effect of the growth of OLs, we only test the travel restrictions imposed when mainland China is the OL from January 21, 2020, to February 22, 2020. We find that ATD/ICR increases as d is negative, indicating the earlier to impose travel restrictions, the more ATD/CIR would be produced, and vice versa. If the selected existing travel restrictions are imposed 14 days later, 0.014 (95% CI, 0.012 to 0.017) fewer days of ATD and 183,510 (95% CI, 29,810 to 1,097,869) fewer cases of ICR would be generated for existing travel restrictions. And 0.13 (95% CI, 0.11 to 0.15) fewer days of ATD and 1,409,822 (95% CI, 114,646 to 19,901,571) fewer cases of ICR would be generated for coordinated travel restrictions. However, if the existing travel restrictions were imposed 14 days earlier, 0.80 (95% CI, 0.60 to 0.94) more days of ATD and 510,438 (95% CI, 98,668 to 2,734,525) more cases of ICR would be generated for the world. Checking the ICR against 6,057,853 infected cases on June 1, 2020, the world would have about 8.4% infected individuals protected from the virus. Specifically, mainland China's lockdown would contribute 0.74 more days of ATD and 417,599 more cases of ICR if it were imposed 14 days earlier. For the coordinated travel restrictions, 0.51 (95% CI, 0.42 to 0.61) more days of ATD and 19,207,427 (95% CI, 950,681 to 419,847,738) more cases of ICR would be generated, providing the possibility of ending the spread of COVID-19 if travel restrictions are implemented in a coordinated way at the very early stage.

Discussion. In summary, we quantify the effectiveness of travel restrictions (i.e., entry ban, global travel ban, and lockdown) concerning COVID-19 by measuring the reduction of airline

traffic as *country distancing increase* and further map the *country distancing increase* to the arrival time delay (ATD) and infected case reduction (ICR). We provide clues for the ineffectiveness and inefficiency of existing travel restrictions, which are premature and lead to an uncontrolled COVID-19 transmission through the analysis. Including the full lockdown imposed by mainland China[27,40,41], which could significantly prevent further exportation of coronavirus to the rest of the world, only 11.36% of travel restrictions are effective. By maximizing travel restrictions' *country distancing increase* and minimizing the loss of airline passenger influx, we find that well deployment of entry bans to OLs with global joint efforts as early as possible is sufficient to fight against COVID-19 effectively. Detailed deployment of optimized travel restrictions enable the sustainable suppression of transmission at a low-level[42], without the need for more radical approaches (e.g., global travel ban), which are harmful to the economy.

Three limitations can lead one to underestimate/overestimate travel restrictions' effectiveness: (1) Incomplete and biased travel restrictions dataset; (2) Homogeneous assumptions on the strengths of different travel restrictions. (3) Ignorance of the combined effect between travel restrictions (international anti-contiguous policies) and local anti-contiguous policy, like social-distancing policy, work from home, and school closure[43,44]. Nevertheless, this study, all the same, provides profound implications that help to stop COVID-19. It offers economical and efficient travel restrictions implementation to slow the spread of COVID-19 while preserving global socio-economic health. Specifically, it recommends that the outbreak locations should impose lockdowns as early as possible. The other geographical areas, which are not outbreak locations, should impose entry bans to outbreak locations as early as possible and tailor their entry bans by tracking OLs'

changes. Furthermore, as the pandemic of COVID-19 is more than a health crisis and may last to 2022[45], geographical areas would continuously endure the coronavirus importation risk from other infected areas and social instability. It is impossible to curb the spread of COVID-19 with travel restrictions imposed by a single region. Thus, this study recommends that the joint global implementation of travel restrictions in a coordinated way as a "whole-of-government" and "whole-of-society" approach is necessary to fight against COVID-19 and strengthen pandemic preparedness for the future[39]. Moreover, our methodology's fundamental advantage is its independence of a disease's epidemiological features and therefore provides insight for strategy preparedness and response plan for seasonal coronaviruses with high mutation rates.

Acknowledgements

Funding This work was supported in part by the Department of Mechanical Aerospace and Nuclear Engineering Department at Rensselaer Polytechnic Institute, Troy, NY.

Author Contributions L.Z., M.D. and J.G. conceived the project and designed the experiments; L.Z. collected the data set and analyzed the data; L.Z. and J.G. carried out theoretical calculations; L.Z. and W.W. performed the experiments on optimizations; L.Z., M.D. and J.G. wrote the manuscript; all authors edited the manuscript.

Competing Interests The authors declare that they have no competing financial interests.

Data and materials availability All data needed to evaluate the conclusions in the paper are presented in this paper. Additional data related to this paper may be requested from the authors.

Additional information Supplementary information including Fig. S1-S11, Tab. S1-S4, Eqs. (S1)-(S28), and Ref. S1-S12.

1. World Health Organization. Coronavirus disease 2019 (covid-19): situation report, 154. Accessed June 22, 2020.

2. The Novel Coronavirus Pneumonia Emergency Response Epidemiology Team. The epidemiological characteristics of an outbreak of 2019 novel coronavirus diseases (covid-19)—china, 2020. *China CDC Weekly* **2**, 113–122 (2020).

3. McCloskey, B. *et al.* Mass gathering events and reducing further global spread of covid-19: a political and public health dilemma. *The Lancet* **395**, 1096–1099 (2020).

4. Dalziel, B. D., Pourbohloul, B. & Ellner, S. P. Human mobility patterns predict divergent epidemic dynamics among cities. *Proceedings of the Royal Society B: Biological Sciences* **280**, 20130763 (2013).

5. Belik, V., Geisel, T. & Brockmann, D. Natural human mobility patterns and spatial spread of infectious diseases. *Physical Review X* **1**, 011001 (2011).

6. Saker, L. *et al.* Globalization and infectious diseases: a review of the linkages. Tech. Rep., World Health Organization (2004).

7. Kucharski, A. J. *et al.* Early dynamics of transmission and control of covid-19: a mathematical modelling study. *The lancet infectious diseases* (2020).

8. Adiga, A. *et al.* Evaluating the impact of international airline suspensions on the early global spread of covid-19. *medRxiv* (2020).

9. Tang, B. *et al.* Estimation of the transmission risk of the 2019-ncov and its implication for public health interventions. *Journal of clinical medicine* **9**, 462 (2020).

10. Pinotti, F. *et al.* Lessons learnt from 288 covid-19 international cases: importations over time, effect of interventions, underdetection of imported cases. *medRxiv* (2020).

11. Sun, J. *et al.* Covid-19: epidemiology, evolution, and cross-disciplinary perspectives. *Trends in Molecular Medicine* (2020).

12. Gonzalez-Reiche, A. S. *et al.* Introductions and early spread of sars-cov-2 in the new york city area. *Science* (2020).

13. Hadfield, J. *et al.* Nextstrain: real-time tracking of pathogen evolution. *Bioinformatics* **34**, 4121–4123 (2018).

14. Wilder-Smith, A. & Freedman, D. Isolation, quarantine, social distancing and community containment: pivotal role for old-style public health measures in the novel coronavirus (2019-ncov) outbreak. *Journal of travel medicine* **27** (2020).

15. Brockmann, D. & Helbing, D. The hidden geometry of complex, network-driven contagion phenomena. *science* **342**, 1337–1342 (2013).

16. Colizza, V., Barrat, A., Barthélemy, M. & Vespignani, A. The role of the airline transportation network in the prediction and predictability of global epidemics. *Proceedings of the National Academy of Sciences* **103**, 2015–2020 (2006).

17. Anderson, R. M., Heesterbeek, H., Klinkenberg, D. & Hollingsworth, T. D. How will country-based mitigation measures influence the course of the covid-19 epidemic? *The Lancet* **395**, 931–934 (2020).

18. Peto, J. *et al.* Universal weekly testing as the uk covid-19 lockdown exit strategy. *The Lancet* **395**, 1420–1421 (2020).

19. Salcedo, A. & Cherelus, G. Coronavirus travel restrictions, across the globe. *The New York Times* (2020).

20. Wikipeida. Travel restrictions related to the 2019–20 coronavirus pandemic. Accessed April 4, 2020.

21. Economist. The new coronavirus could have a lasting impact on global supply chains. Accessed April 4, 2020.

22. Habibi, R. *et al.* Do not violate the international health regulations during the covid-19 outbreak. *The Lancet* **395**, 664–666 (2020).

23. Ferretti, L. *et al.* Quantifying sars-cov-2 transmission suggests epidemic control with digital contact tracing. *Science* (2020).

24. Heymann, D. The need for a coordinated international pandemic response. *Bull World Health Organ* **98**, 378–379 (2020).

25. Mateus, A. L., Otete, H. E., Beck, C. R., Dolan, G. P. & Nguyen-Van-Tam, J. S. Effectiveness of travel restrictions in the rapid containment of human influenza: a systematic review. *Bulletin of the World Health Organization* **92**, 868–880D (2014).

26. Dehning, J. *et al.* Inferring change points in the spread of covid-19 reveals the effectiveness of interventions. *Science* (2020).

27. Chinazzi, M. *et al.* The effect of travel restrictions on the spread of the 2019 novel coronavirus (covid-19) outbreak. *Science* (2020).

28. Li, R. *et al.* Substantial undocumented infection facilitates the rapid dissemination of novel coronavirus (sars-cov-2). *Science* **368**, 489–493 (2020).

29. Lau, H. *et al.* Internationally lost covid-19 cases. *Journal of Microbiology, Immunology and Infection* (2020).

30. Russel, T., Hellewell, J., Abbot, S. *et al.* Using a delay-adjusted case fatality ratio to estimate under-reporting. *Available at the Centre for Mathematical Modelling of Infectious Diseases Repository, here* (2020).

31. Jiang, C., Gao, J. & Magdon-Ismail, M. True nonlinear dynamics from incomplete networks. In *Proceedings of the AAAI Conference on Artificial Intelligence*, vol. 34, 131–138 (2020).

32. Mangili, A. & Gendreau, M. A. Transmission of infectious diseases during commercial air travel. *The Lancet* **365**, 989–996 (2005).

33. Jia, J. S. *et al.* Population flow drives spatio-temporal distribution of covid-19 in china. *Nature* 1–11 (2020).

34. Iannelli, F., Koher, A., Brockmann, D., Hövel, P. & Sokolov, I. M. Effective distances for epidemics spreading on complex networks. *Physical Review E* **95**, 012313 (2017).

35. Lin, S., Huang, J., He, Z. & Zhan, D. Which measures are effective in containing covid-19? empirical research based on prevention and control cases in china. *medRxiv* (2020).

36. https://ourworldindata.org/grapher/covid-confirmed-cases-since-100th-case.

37. Anderson, R. M. & May, R. M. *Infectious diseases of humans: dynamics and control* (Oxford university press, 1992).

38. Li, Q. *et al.* Early transmission dynamics in wuhan, china, of novel coronavirus–infected pneumonia. *New England Journal of Medicine* (2020).

39. World Health Organization. Covid-19 strategy update (2020).

40. Kraemer, M. U. *et al.* The effect of human mobility and control measures on the covid-19 epidemic in china. *Science* (2020).

41. Tian, H. *et al.* An investigation of transmission control measures during the first 50 days of the covid-19 epidemic in china. *Science* (2020).

42. Ruktanonchai, N. W. *et al.* Assessing the impact of coordinated covid-19 exit strategies across europe. *Science* (2020).

354 43. Hsiang, S. *et al.* The effect of large-scale anti-contagion policies on the covid-19 pandemic.
355 *Nature* 1–9 (2020).

356 44. Aleta, A. *et al.* Modelling the impact of testing, contact tracing and household quarantine on
357 second waves of covid-19. *Nature Human Behaviour* 1–8 (2020).

358 45. Kissler, S. M., Tedijanto, C., Goldstein, E., Grad, Y. H. & Lipsitch, M. Projecting the trans-
359 mission dynamics of sars-cov-2 through the postpandemic period. *Science* (2020).

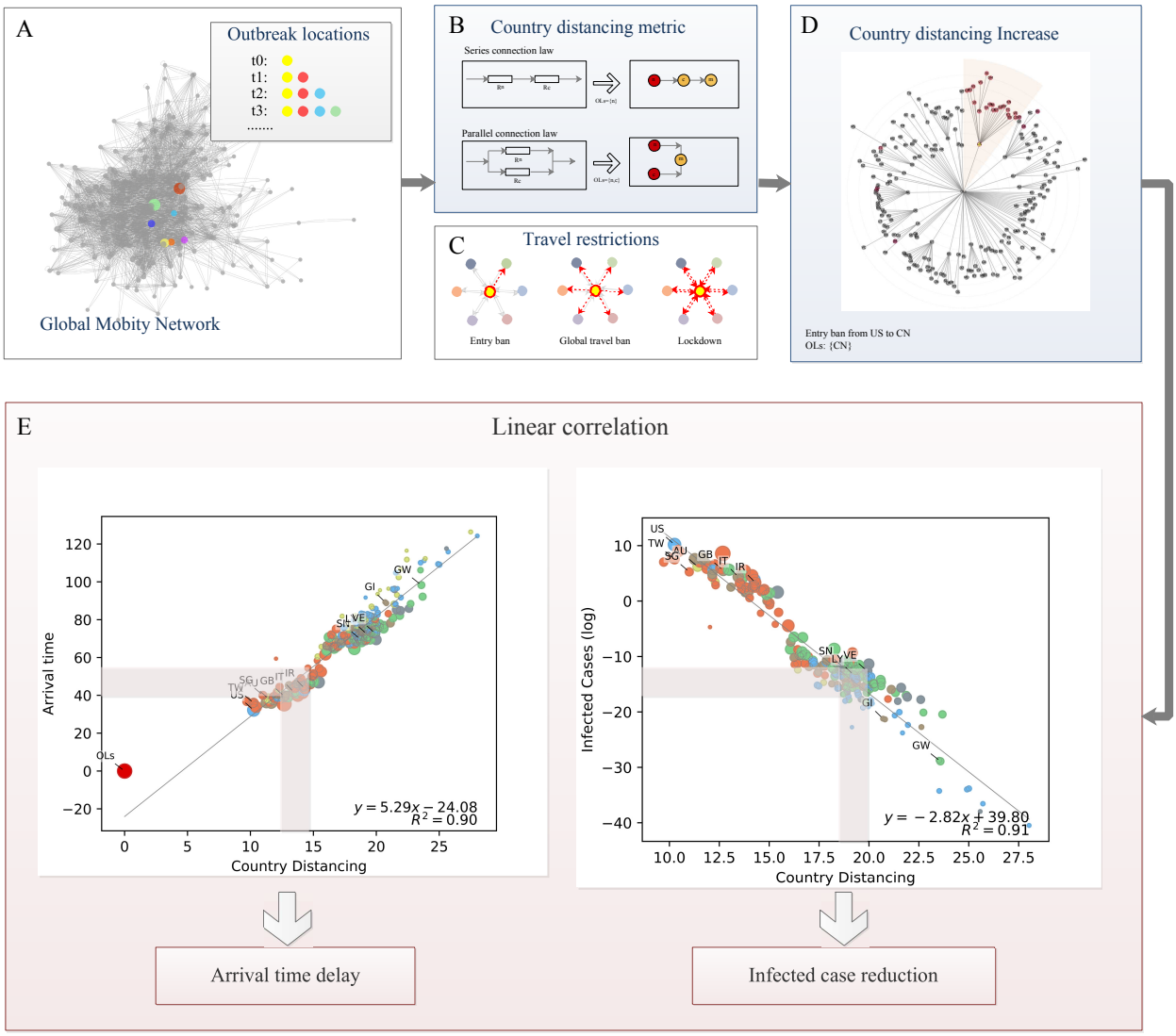

Figure 1: Understanding how the changes in global mobility network caused by travel restrictions are mapped to arrival time delay (ATD) and infected case reduction (ICR) for geographical areas through country distancing metric. (A) Global mobility network (GMN) and growing outbreak locations. (B) Series and parallel connection law for country distancing metric. (C) Ways of travel restrictions, i.e., entry ban, global travel ban, and lockdown, reduced passenger influx from GMN. (D) Visualization of shortest path tree to show the *country distancing increase* at geographical area. The geographical area is marked in red if it has *country distancing increase*. (F) Mapping *country distancing increase* to ATD and ICR through the linear correlations between country distancing with arrival times and log-transformed infected cases. Each dot represents the geographical area. The geographical areas belonging to the same continent are in the same color.

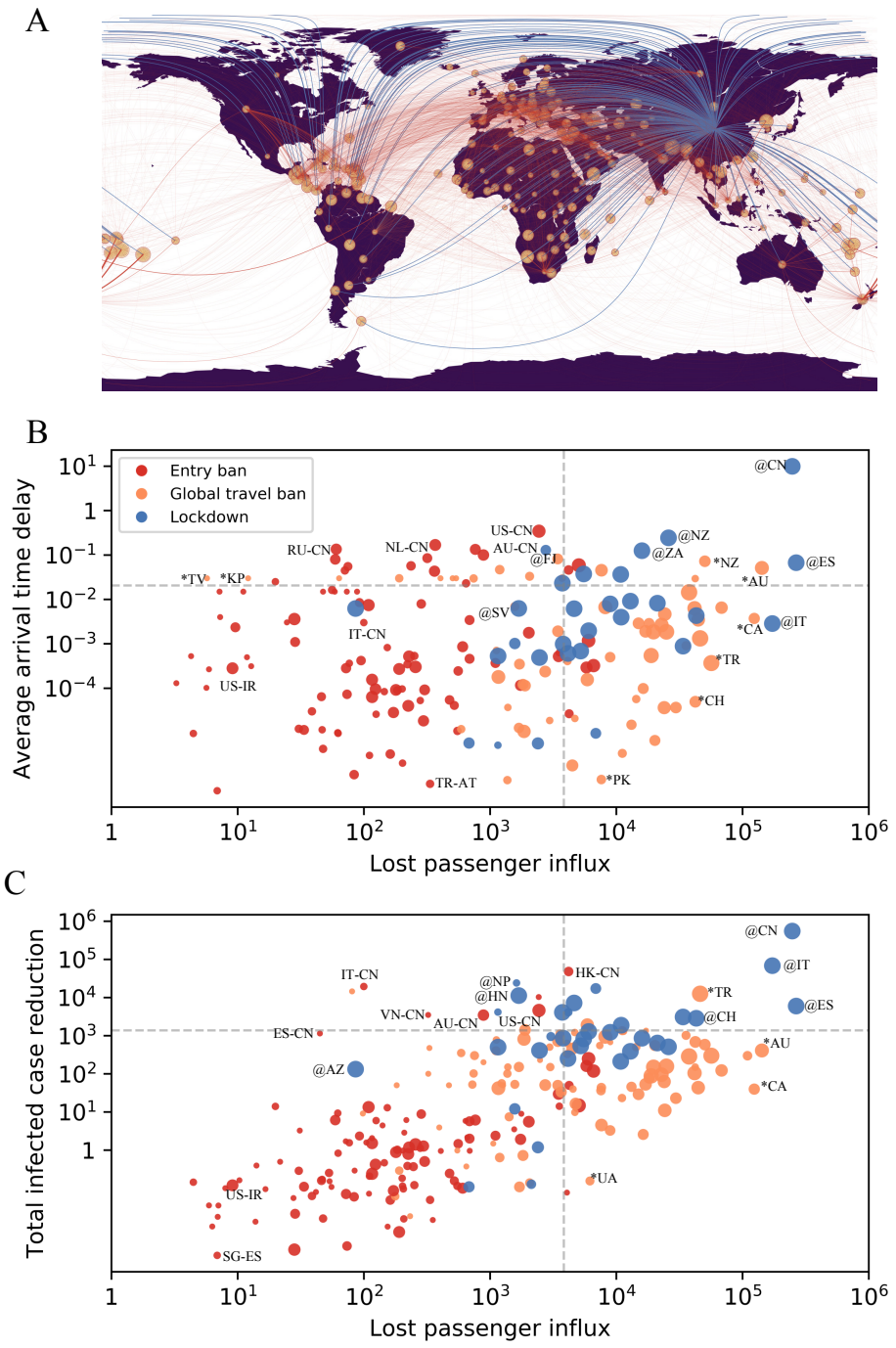

Figure 2: Effectiveness and efficiency of existing travel restrictions. (A) Overview of existing travel restrictions' impact on each geographical area. The size of circle at each area is proportional to its *country distancing increase*. The curved lines depict the effort of travel restrictions from one area to another area. (B)(C) Existing travel restrictions' arrival time delay (B) and infected case reduction (C) at the cost of losing passenger influx. The dot size is proportional to the number of influenced geographical areas, whose country distancing raise due to the travel restriction. Among the marks, for example, the "US-CN" represents the entry ban imposed by US to CN (mainland China); "*KP" represents the global travel ban imposed by North Korea; "@CN" represents the lockdown imposed by mainland China. For clear visualization, geographical areas are presented by two-letter codes.

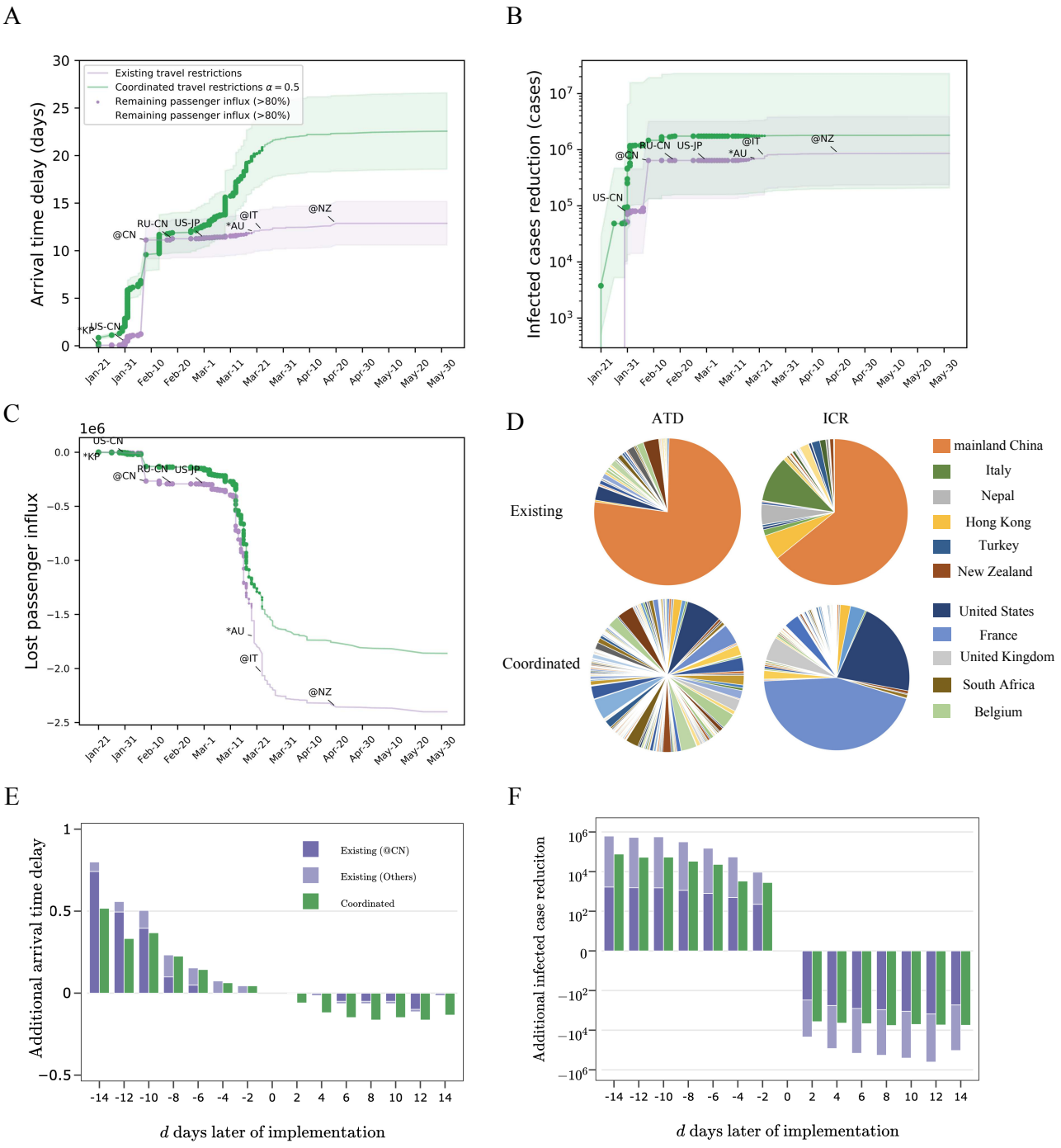

Figure 3: Optimized travel restrictions, which are deployed in an coordinated approach, in comparison to existing travel restrictions in six manners. The six manners are arrival time delay (A) and infected case reduction (B), lost passenger influx (C), geographical area' contribution in inducing arrival time delay and infected case reduction by imposing travel restrictions (D), and additional average arrival time delay (E) and total infected case reduction (F) if the selected travel restrictions' occurrence dates are d days after original occurrence date. Here, $d < 0$ implies that the travel restrictions are imposed d day earlier than original occurrence date. Each coordinated and targeted solution of travel restriction, which comprises a set of coordinated entry bans, is the non-dominated solution with NSGA- II.

Figures

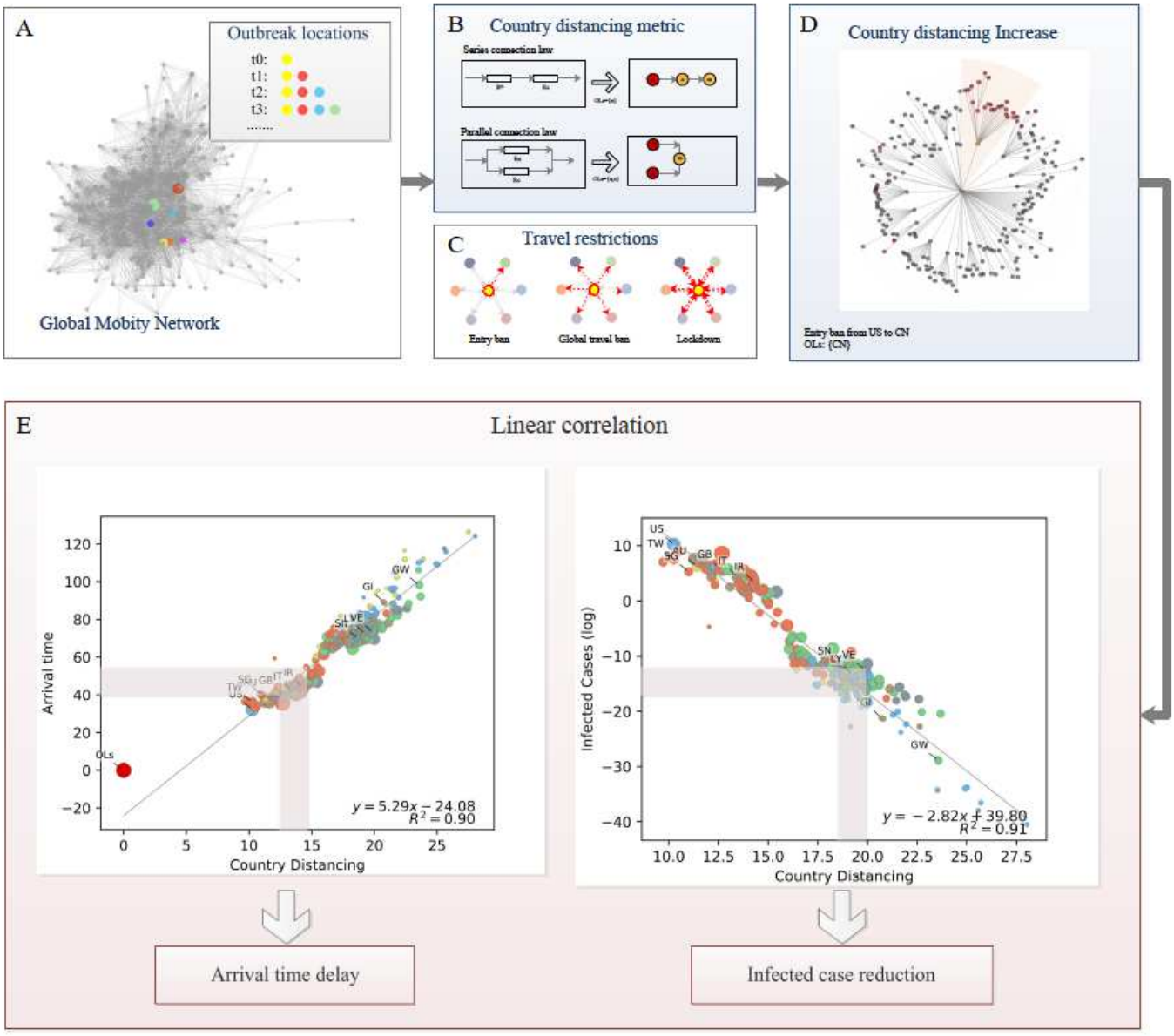

Figure 1

Understanding how the changes in global mobility network caused by travel restrictions are mapped to arrival time delay (ATD) and infected case reduction (ICR) for geographical areas through country distancing metric. (A) Global mobility network (GMN) and growing outbreak locations. (B) Series and parallel connection law for country distancing metric. (C) Ways of travel restrictions, i.e., entry ban, global travel ban, and lockdown, reduced passenger influx from GMN. (D) Visualization of shortest path tree to show the country distancing increase at geographical area. The geographical area is marked in red if it has country distancing increase. (F) Mapping country distancing increase to ATD and ICR through the linear correlations between country distancing with arrival times and log-transformed infected cases.

Each dot represents the geographical area. The geographical areas belonging to the same continent are in the same color.

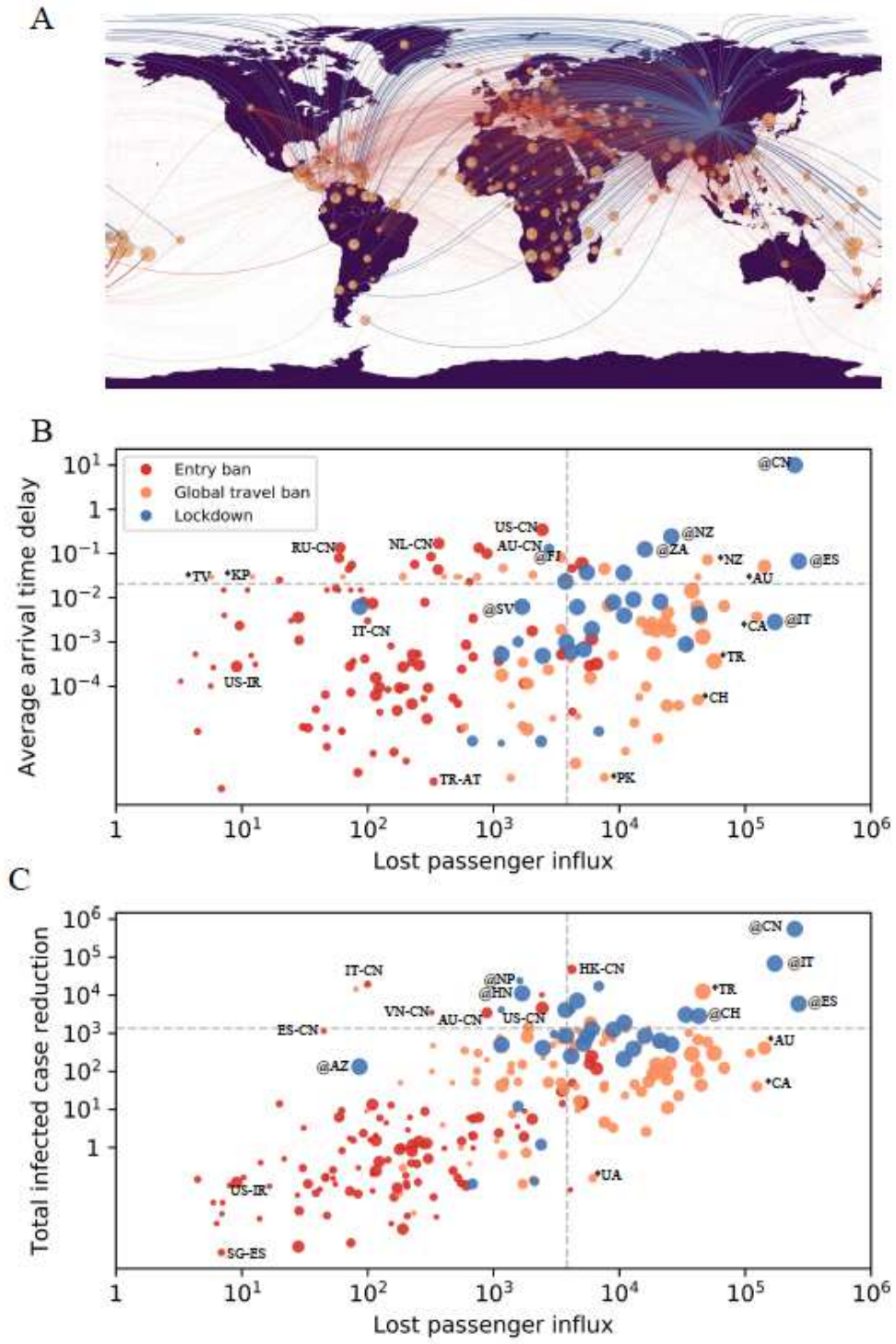

Figure 2

Effectiveness and efficiency of existing travel restrictions. (A) Overview of existing travel restrictions' impact on each geographical area. The size of circle at each area is proportional to its country distancing increase. The curved lines depict the effort of travel restrictions from one area to another area. (B)(C)

Existing travel restrictions' arrival time delay (B) and infected case reduction (C) at the cost of losing passenger influx. The dot size is proportional to the number of influenced geographical areas, whose country distancing raise due to the travel restriction. Among the marks, for example, the "US-CN" represents the entry ban imposed by US to CN (mainland China); "*KP" represents the global travel ban imposed by North Korea; "@CN" represents the lockdown imposed by mainland China. For clear visualization, geographical areas are presented by two-letter codes. Note: The designations employed and the presentation of the material on this map do not imply the expression of any opinion whatsoever on the part of Research Square concerning the legal status of any country, territory, city or area or of its authorities, or concerning the delimitation of its frontiers or boundaries. This map has been provided by the authors.

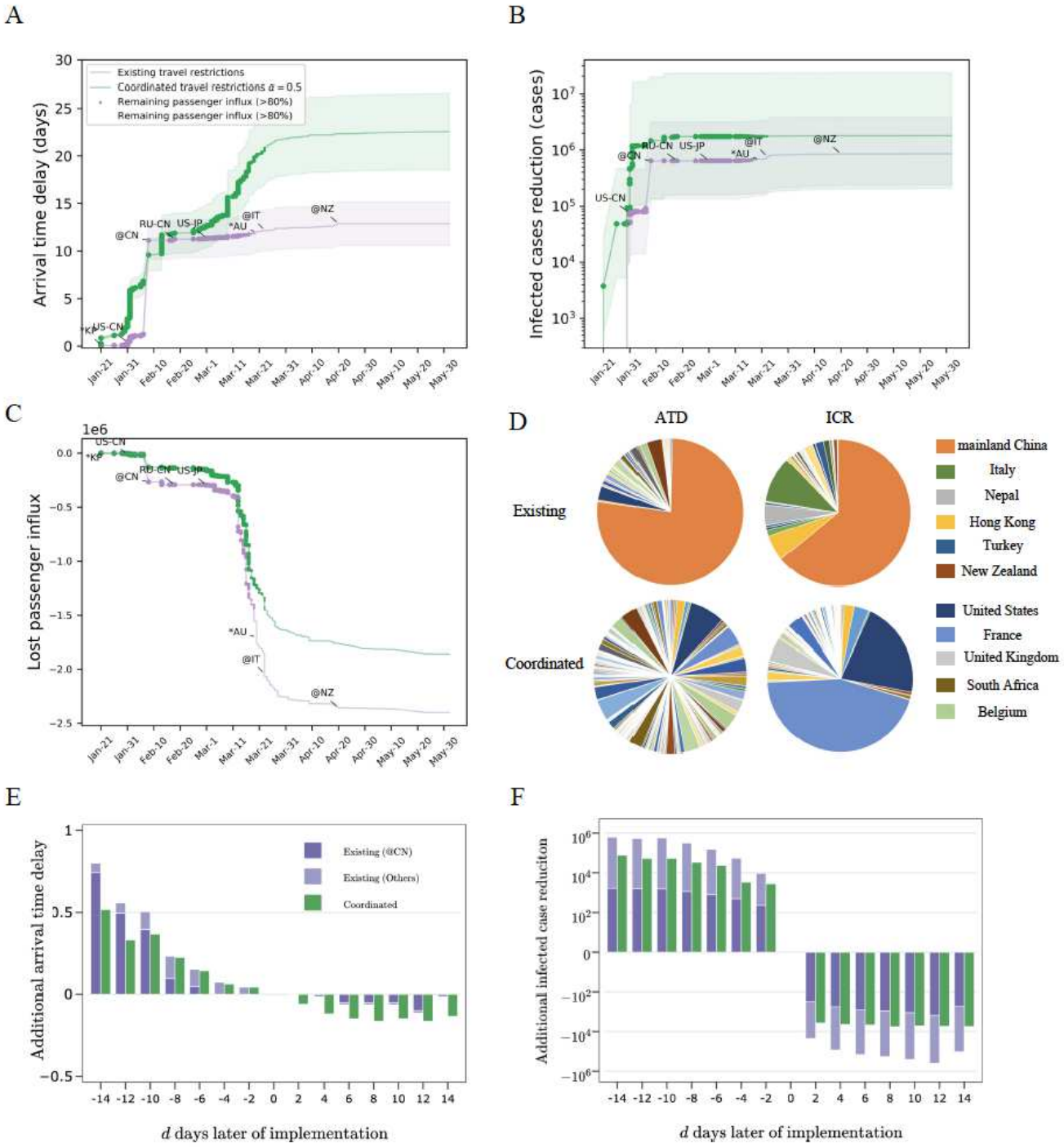

Figure 3

Optimized travel restrictions, which are deployed in an coordinated approach, in comparison to existing travel restrictions in six manners. The six manners are arrival time delay (A) and infected case reduction (B), lost passenger influx (C), geographical area' contribution in inducing arrival time delay and infected case reduction by imposing travel restrictions (D), and additional average arrival time delay (E) and total infected case reduction (F) if the selected travel restrictions' occurrence dates are d days after original occurrence date. Here, d < 0 implies that the travel restrictions are imposed d day earlier than original

occurrence date. Each coordinated and targeted solution of travel restriction, which comprises a set of coordinated entry bans, is the non-dominated solution with NSGA- II.

Supplementary Files

This is a list of supplementary files associated with this preprint. Click to download.

- Supplementary.pdf